



Fracture Toughness of Glass infiltrated (3Y-TZP/Al₂O₃) Composite

Sara N. Ibrahim^{a*}, Shihab A. Zaidan^b, Mudhafar A. Mohammed^c

^a Department of Applied Sciences, University of Technology, Baghdad, Iraq,
102180@student.uotechnology.edu.iq

^b Department of Applied Sciences, University of Technology, Baghdad, Iraq, 100160@uotechnology.edu.iq

^c Department of Applied Sciences, University of Technology, Baghdad, Iraq, 100167@uotechnology.edu.iq

*Corresponding author.

Submitted: 11/11/2020

Accepted: 13/12/2020

Published: 25/03/2021

KEY WORDS

ATZ-glass composite
Fracture toughness, 3Y-TZP, Brittleness index.

ABSTRACT

Five different 3 mol.% yttria-tetragonal zirconia polycrystals/alumina (3Y-TZP/Al₂O₃)-glass specimens have been fabricated by the glass infiltration method. Graphite additives were added to the (3Y-TZP/20Wt.%Al₂O₃) to obtain porous structure. The ATZ (Alumina Toughened Zirconia) skeleton has been prepared by the normal compaction method. The specimen has been infiltrated by the glass (18Wt.% lithium hydroxide, 72 wt. % feldspar, and 10Wt.% nano Titanium oxide) at 1185°C. Results showed that the porosity of (3Y-TZP/Al₂O₃) composite was increased while bulk density decreased with increasing graphite additives. The elastic modulus of (3Y-TZP/Al₂O₃)-glass was decreased (159-109GPa) with increasing the amount of glass infiltrated. Hardness was constant for all the specimens in value of (5.66 GPa), while increment of materials fracture toughening was due to the increasing the glass weight fraction, the k_{Ic} was lied between (0.53-1.54MPa.m^{1/2}). The glass infiltrated (3Y-TZP/Al₂O₃) process was successfully increased the fracture toughness by penetrated different amounts of glass into the (3Y-TZP/Al₂O₃) structure.

How to cite this article: S. N. Ibrahim, S. A. Zaidan, and M. A. Mohammed, "Fracture Toughness of Glass infiltrated (3Y-TZP/Al₂O₃) Composite," Engineering and Technology Journal, Vol. 39, Part B, No. 01, pp. 141-149, 2021.

DOI: <https://doi.org/10.30684/etj.v39i1B.1919>

This is an open access article under the CC BY 4.0 license <http://creativecommons.org/licenses/by/4.0>

1. INTRODUCTION

The construction of all-ceramic restorations was demonstrated by several all-ceramic systems. Among these, the most popular examples are glass-ceramics, leucite-reinforced porcelains, polycrystalline ceramics and glass-infiltrated ceramic composites [1]. Brittleness inherited into ceramics and poor ability to undergo plastic deformation were the main disadvantage of all-ceramic restorations because it causes failure in clinical trials due to the high fracture rates [2]. In order to

understand ceramic restorations fracture behavior, light must be shed on fracture mechanics causes of the process. Extrinsic and intrinsic flaws exist in all-ceramic components, knowing the size of the flaw which can be tolerated in the structure and the lifetime of the structure containing defect is very important. In 1913, the first work about the action of the defect as a stress concentration was published by Inglis [3] who demonstrated that sharp cracks are deleterious much more than one with blunt cracks. Griffith, in the 1920s, established the relation between crack size and fracture strength [4]. For ductile materials, Griffith's original work had to be later modified by Irwin [5]. The suggestion of Irwin was that the equation of Griffith must be written again and add the energy of elastic deformation accompanied the process of fracture. For that reason, he chose the G parameter, considering the rate of releasing strain energy. The fracture process was greatly understood by Griffith's approach. But other methods studied fields of stress which is close to the tip of cracks. This crack can be considered as a stress intensity factor called (K). In 1958, Irwin associated the concepts of Inglis and Griffith and showed that the strain energy release rate (G) is a function of the stress intensity factor (K) [6]. Rearranging Griffith's equation, the stress intensity factor at the crack tip (K_I , I denote uniaxial tensile or opening mode), which is also called K_{IC} (critical stress intensity factor), is related to the stress at fracture in mode I according to the equation [7].

$$K_{IC} = \sigma_f Y \sqrt{a} \quad (1)$$

where Y is a dimensionless constant that depends on the loading mode, dimensions of the material, shape, geometry and length of the crack. a is the length of the crack from which the fracture propagates. K_{IC} is a constant for a given material and is commonly referred to as fracture toughness. Eq. (1) can also be considered a failure criterion since the brittle fracture of the material will occur when the product of the stress applied by the square root of a crack size is equal to or greater than the material's fracture toughness value.

Fracture toughness and young modulus are very important properties for dental ceramics. The reversible deformation amount which happened in a structure by an applied load to it was considered an indication of elastic modulus. The resistance of pulling atoms that are adjacent can be expressed by interatomic spacing small changes due to the band stretching [8]. The ability of the material to absorb energy from the elastic deformation, accompanied to the tensile stress level which can be achieved before catastrophic fracture initiation near the crack tip was defined as fracture toughness. Because dental ceramic is similar to all brittle materials by an ability to absorb a good quantity of elastic strain energy before fracture, in this case, the fracture toughness can be expressed by measuring the ability to absorb strain energy for brittle material [9].

The main object of this study was to determine the effect of the glass amount infiltrated into the ceramic structure on the fracture toughness of 3Y-TZP/ Al_2O_3 .

2. EXPERIMENTAL

I. Preparation of (3Y-TZP)/ Al_2O_3

3 mol.% yttria (sky spring nanomaterials, USA) was added to zirconia fine commercial powder (Riedel de Haen, Germany, purity 99, particle size $<5 \mu m$) to produce 3Y-TZP. Fine powder of 3Y-TZP then mixed with 20Wt.% nano Al_2O_3 (α - Al_2O_3 purity $>99/99\%$, the average particle size of 13 nm, sigma Aldrich, U.S.A) to prepare (3Y-TZP)/ Al_2O_3 . Graphite particles (32) μm supplied by "State Company of Geological Survey and Mining" added to ATZ (Alumina Toughened Zirconia) in various Wt.% (0,10,20,30,40) to prepare porous specimens. The powder mixture pressed uniaxially in a steel die for 30 sec. to form pellets of (10 mm diameter and 5 mm thickness).

II. Preparation of Lithium silicate glass.

The glass powder mixture was prepared by mixing 18 Wt.% Lithium Hydroxide (manufactured by Strem Chemicals, inc. USA) with 72 Wt. % feldspar (brought from State Company of Geological Survey and Mining-Iraq), and 10 Wt.% Nano titanium dioxide ($>26nm$, purity 99.8% supplied by Cheng Du Micxy Chemical Co. Ltd-China). Lithium Hydroxide first dissolved in distilled water by using a magnetic stirrer, feldspar and nano TiO_2 then added to the solution and mixed for 3hrs to achieve homogenization.

III. Preparation of (3Y-TZP)/Al₂O₃- glass.

Water was mixed with a powder mixture of a glass to form glass slurry, the slurry has been pasted in a uniform way to coat the (3Y-TZP/Al₂O₃) specimen's all surfaces. Then dried in an oven at 50 °C. Subsequently, a programmable electrical furnace (type NABERTHERM-P310-GERMANY) was used to heated specimens in the air with the temperature rising rate 17min/°C up to 1185°C with a soaking time of 150 minutes. At a certain temperature, the glass melted and started the infiltration process according to the principle of capillarity action.

IV. Testing

1. Physical Properties (Porosity and Bulk Density) for (3Y-TZP/Al₂O₃).

Archimedes principle used to calculate the Apparent porosity (A.P) and Bulk density (B.D) of (3Y-TZP/ Al₂O₃) composite after sintering at 1500°C as follows:

$$A.P \% = \frac{W_s - W_d}{W_s - W_i} \times 100 \quad (2)$$

$$B.D (g/cm^3) = \frac{W_d}{W_s - W_i} \quad (3)$$

Where, W_d: The dry sample mass, W_s: The sample being infiltrated with water mass, and W_i: The sample is immersed in water mass.

2. Mechanical properties of (3Y-TZP/ Al₂O₃)-Glass

1) Elastic modulus.

An ultrasonic device type (GE USM 35x) used as a non-destructive test for the determination of young modulus. This device operated on pulse-echo mode. 3 different frequencies of prob (1,2 and 4MHz) are used. The thickness of (3y-TZP)-glass was calculated. This test was based on measuring the time of flight of ultrasonic waves through materials with known thickness. The data have been processed in the device to determine ultrasonic wave velocity. Three different spots were conducted through testing. Modulus of elasticity estimated using the following equations:

$$E(GPa) = \frac{V_l \rho (1 + \nu)(1 - 2\nu)}{1 - \nu} \quad (4)$$

$$\nu = \frac{(1 - 2b)^2}{(2 - 2b)^2} \quad (5)$$

Where elastic modulus referred by E, the velocity of the ultrasonic wave in the longitudinal direction referred by V_l, the bulk density referred by ρ, and the material's Poisson's ratio referred by ν. While b= V_s/ V_l respectively [10].

2) Hardness and Fracture toughness.

Measuring Vickers hardness and the fracture toughness (K_{IC}) and the Vickers hardness (HV) accomplished using the digital microhardness tester type LARYEE - HVS-1000/HVS-1000Z. 9.8 N was the applied load to obtain Vicker's indentation, the load was held for (30) seconds. To increase the accuracy, 3 measurements were taken for each sample and the average was calculated HV and K_{IC} were estimated by [11]:

$$H = \frac{P}{\alpha \cdot a^2} \quad (6)$$

$$K_{Ic} = \frac{\zeta \left(\frac{E}{H}\right)^{\frac{1}{2}} \cdot P}{C^{\frac{3}{2}}} \tag{7}$$

Where: H is Vickers hardness (GPa), p is the load(N), α is indenter shape-dependent called numerical factor for Vickers hardness $\alpha = 2$, a is the indenter length(m). K_{Ic} is the fracture toughness ((MPa.m^{1/2}), ζ is a dimensionless constant, which for ceramics has an average value of $0.016 \pm 0.004E$ is the young modulus (GPa), C is the indentation crack lengths (mm). Figure (1) shows the crack at an indent used in fracture toughness calculation.

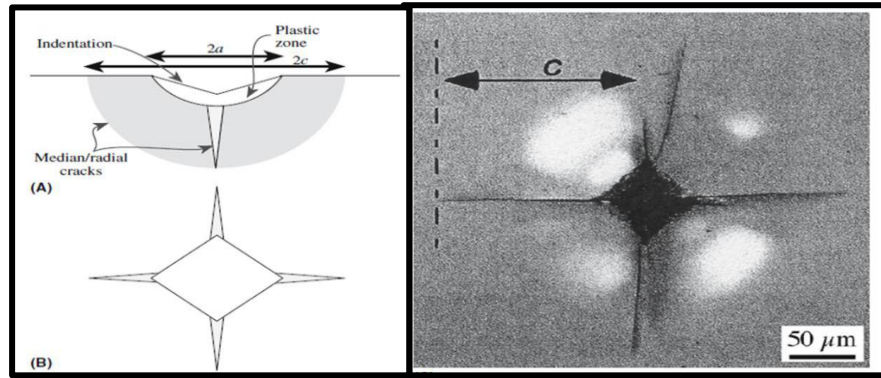


Figure 1: Cracks at an indent allow determination of K_{Ic} .

3. RESULTS AND DISCUSSION

Figure (2) shows the relation between graphite additives with apparent porosity and bulk density for (3Y-TZP/Al₂O₃) before glass infiltration. It's showed that as the amount of graphite increased, the apparent porosity increases while bulk density decreased. The porosity determination test is important to understand the ability of the material to infiltrated by the glass through capillarity action. By calculation of specimens' weight before and after infiltration, it was noted that the glass weight % increased with the increment in porosity due to the capillary action. Figure (3) shows the effect of ATZ porosity on the glass weight fraction infiltrated into the ceramic skeleton.

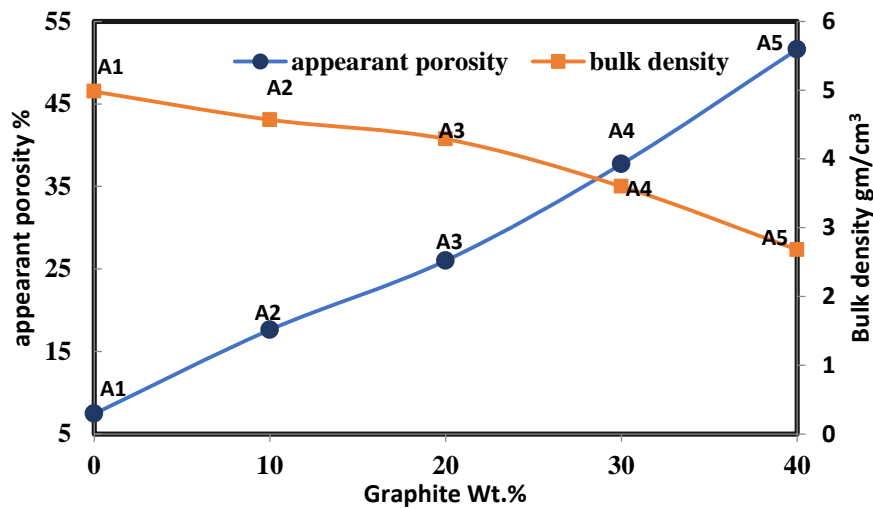


Figure 2: Variation of apparent porosity % and bulk density of (3Y-TZP/Al₂O₃)-with graphite additives.

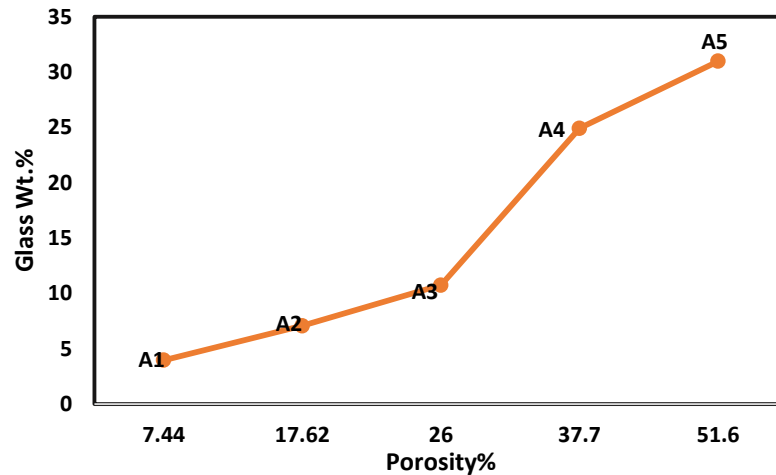


Figure 3: Variation of glass Wt.% of (3Y-TZP/Al₂O₃)-glass with ATZ porosity %.

Young modulus for ATZ after infiltration with lithium silicate glass was shown in figure (4). It can be seen that the value of young modulus for (3Y-TZP/Al₂O₃)-glass was decreased with increasing porosity portion which existed in ATZ skeleton before infiltration. The young modulus for A1 was (195) while A5 was (109). This can be attributed to the increasing in the portion of glass material as a reinforcing phase into the (3Y-TZP/Al₂O₃) Skeleton because appropriate glass infiltration reduces the elastic modulus (Zhang and Kim 2009) [12]. Adding glass to the (3Y-TZP/Al₂O₃) structure will lowering the young modulus and then lower the stiffness within the elastic range when tensile or compressive forces are applied [7]. The young modulus values were agreed with other ceramics reported by Humberto Naoyuki Yoshimura (elastic modulus for leucite-based glass-ceramic (Ivoclar Vivadent/IPS Empres1) was 66.1 GPa (and glass-ceramic with Lithium disilicate (Ivoclar Vivadent/IPS Empres2) was 99.3 GPa. [13]

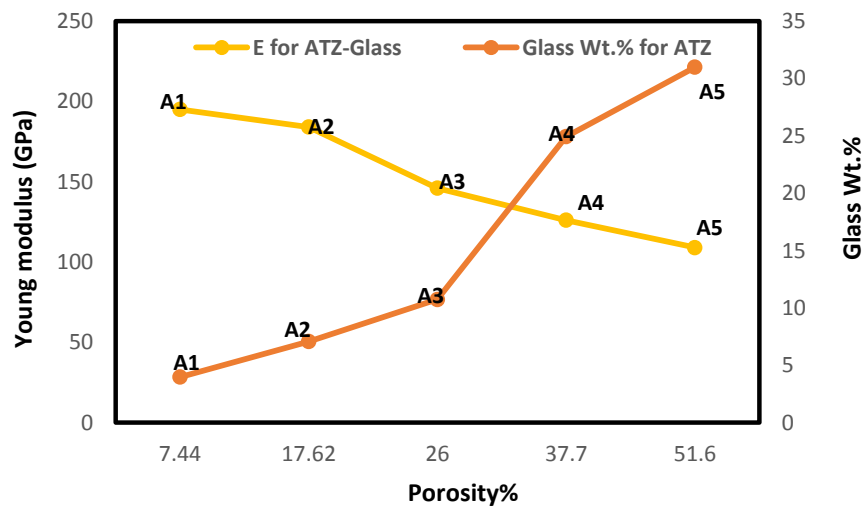


Figure 4: Variation of (3Y-TZP/Al₂O₃)-Glass Young modulus with (3Y-TZP/Al₂O₃) porosity% and glass Wt.%

An optical microscope image shown in figure (5) were it used to determine the dimensions of the Vickers indentation and the length of the crack to calculate (3Y-TZP/Al₂O₃)-glass composite fracture toughness. Values of indentation length, crack length, hardness and toughness are listed in Table 1. The crack length (a) value is the same for the specimens per the group, (a) value is (0.02941mm), as a result, The Vickers hardness values remained constant (HV=5.6644 GPa) and not affected by the amount of glass infiltrating into the structure, probably because Hardness is a surface property that deals with the resistance provided against indentation[14], and as the surface of specimens had the same composition, the hardness value remained constant. No correlation was observed between Vickers hardness and Young’s modulus indicating that the decrease in elastic modulus with porosity which leads to increasing glass Wt.% did not cause an increase in the hardness value. The hardness

values agreed with other ceramics reported by Humberto Naoyuki Yoshimura (HV for leucite-based glass-ceramic (Ivoclar Vivadent/IPS Empres1) was 7.9 GPa (and glass-ceramic with Lithium disilicate (Ivoclar Vivadent/IPS Empres2) was 5.8 GPa [13].

TABLE I: Values of indentation length, crack length, hardness and toughness for (3Y-TZP/Al₂O₃)-Glass.

Specimen	c (mm)	K _{IC} (MPa.m ^{1/2})
A1	0.145098	0.53265
A2	0.098039	0.93159
A3	0.086275	1.00524
A4	0.062745	1.50568
A5	0.058824	1.54278

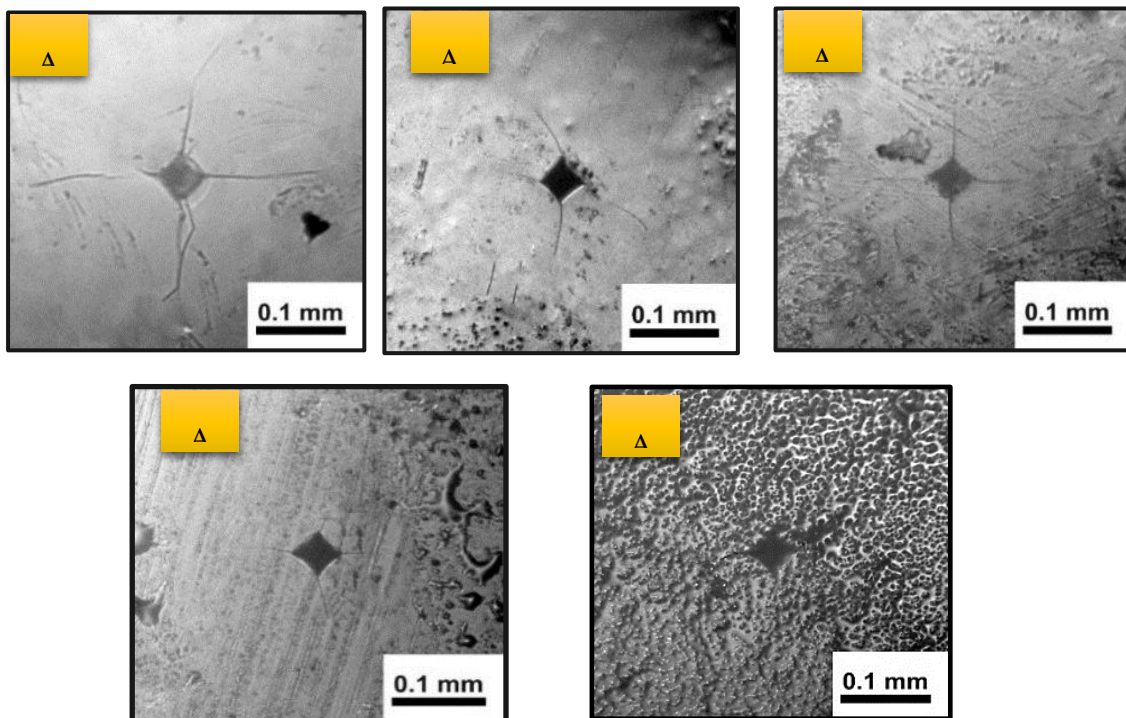


Figure 5: Crack patterns used for hardness and fracture toughness calculations for (3Y-TZP/Al₂O₃)-Glass.

The fracture toughness of specimens is shown in figure (5) while the relation between porosity content in ATZ and fracture toughness of resulted ATZ-glass composite is shown in figure(6). During the indentation, the crack lengths(c) on the glass-infiltrated samples were significantly decreasing with increasing the glass amount infiltrated into the ATZ skeleton, led to increasing the presence of compression stresses in ATZ-glass specimens.

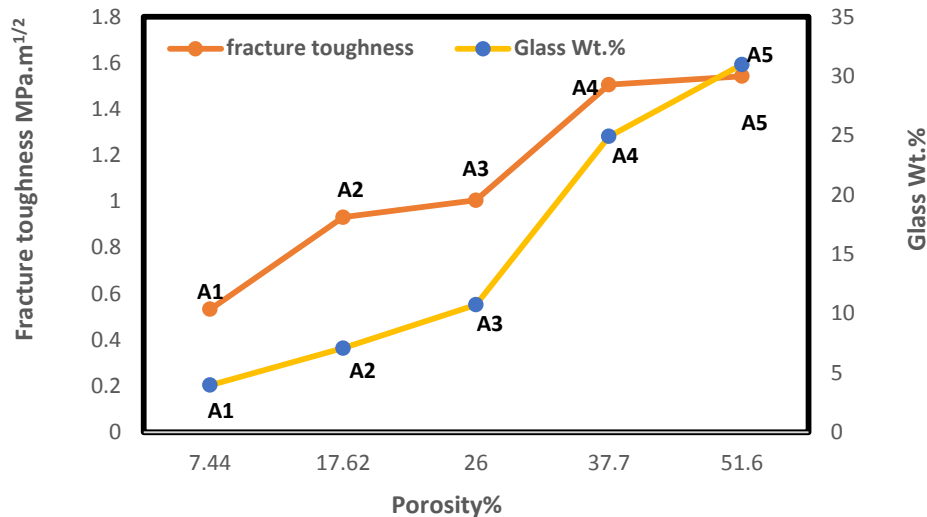


Figure 6: Variation of (3Y-TZP/Al₂O₃)-Glass) Fracture toughness with (3Y-TZP/Al₂O₃) porosity% and Glass Wt.%

The glass-infiltrated sample could be considered as a bi-layer system, having a coating of (3Y-TZP/Al₂O₃)-glass composite on ATZ substrate.

During the coating, the coating will contain stresses these stresses would be generated due to the mismatching in properties (elastic and thermal) resulted between (a) the glass and the ATZ within the composite film (assumed stress equal in all direction) and (b) the (ATZ) substrate which is the naturally biaxial and composite film (ATZ-glass) [15]. Another reason is due to the elastic and thermal expansion (a) mismatch between the ATZ skeleton and the glass. There will be a presence of residual stresses [14]. Several mechanisms contributed to the toughness of (3Y-TZP/Al₂O₃)- glass composites, which can be summarized by deflection, bowing, bridging. Of the crack nonplanar crack can be produced by the crack front deflection around (3Y-TZP/Al₂O₃) particles, this would increase toughness.

Toughness can be enhanced by deflection of the crack because the crack tip stress intensity is reduced. This theory was according to Faber and Evans Model. The toughness can be increased also by crack front bowing between zirconia- alumina particles and this will produce a planar crack [16]. Particle shape and content are the sensitive parameters affected on the crack deflection and bowing. Crack bridging occurs when grains bridge a newly formed fracture surface, creating a restraining force near the crack tip. As the crack extends, energy may be dissipated by friction between the bridging grains and adjacent materials.

These mechanisms could be enhanced due to the presence of residual stresses by the thermal expansion (a) mismatch between the alumina skeleton and the glass, which was investigated by Fisher et al. [18]. The fracture toughness values of resulted (3Y-TZP/Al₂O₃)-Glass were agreed with the other ceramics reported by Humberto Naoyuki Yoshimura (For the two porcelains and the leucite-based glass-ceramic, the K_{IC} values (0.67, 0.84 MPa.m^{1/2}) were similar to the ones reported in the literature for glasses and glass-ceramics with less than 40% in volume of second phase particles (between 0.65-0.87 MPa.m^{1/2}).[13]

The brittleness index (B), which takes into consideration the deformation and fracture resistance, was calculated using the following equation [19]:

$$B = \frac{HV}{K_{Ic}} \quad (8)$$

Where HV is the Vickers hardness, K_{Ic} is the fracture toughness.

By increasing this index, the brittleness increased. All (3Y-TZP/Al₂O₃)- glass specimens were tested and the mean values of B were calculated and shown in figure.6 The B values were observed for (3Y-TZP/Al₂O₃)- glass composite specimens ranging from (10.5-3.63 μm^{-1/2}). The calculated values were lower than those reported for other ceramics (12.2, 9.5 and 8.2 μm^{-1/2} for Vita Zahnfabrik/VM7, Ivoclar Vivadent/d. And Sign Ivoclar Vivadent/IPS Empress, respectively) [13]. A

weak correlation between B values and E were observed, but an inverse correlation with the weight fraction of the glass into (3Y-TZP/ Al_2O_3)- was noticed. Fig. (7) Shows that the values of B reduces as the glass amount increases in the (3Y-TZP/ Al_2O_3)- Skeleton, B for A1 is higher than A5. This result suggests that the brittleness index (B) would be related to the fracture surface energy,

The brittleness index is more efficient in situations involved wear, scratch, machining and erosion in all-ceramic materials. [20]

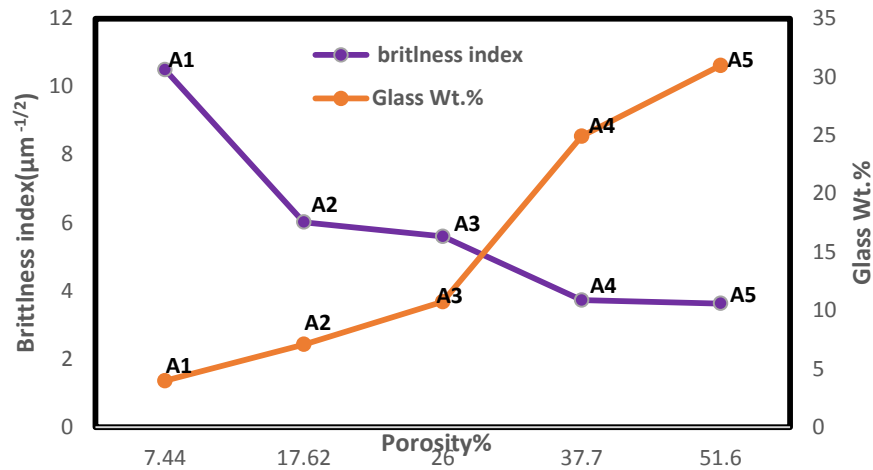


Figure 7: Variation of (3Y-TZP/ Al_2O_3)-Glass Brittleness index with (3Y-TZP/ Al_2O_3) porosity% and Glass Wt. %

4. CONCLUSION

3Y-TZP/ Al_2O_3 -glass specimen was successfully fabricated by glass infiltration ceramic method. The specimens with a higher amount of porosity showed a decrease in young modulus as the glass amount in the final structure will be increased. While the same specimen will show a higher fracture toughness value due to the decrease in the indentation crack length. The increase in toughness resulted from the toughening mechanisms offered by the glass. Increasing the fracture toughness means the fracture surface energy was increased and as a consequence, the brittleness index decreased. The fracture toughness values lie in the range used in other restorative materials. No correlation was observed between Vickers hardness and Young's modulus indicating that the decrease in elastic modulus with increasing porosity and glass Wt.% did not cause an increase in the hardness value. It can be concluded that the A5 specimen had an acceptable combination between fracture toughness ($1.542 \text{ MPa}\cdot\text{m}^{1/2}$) and young modulus (109GPa) with the lowest brittleness index ($3.63 \mu\text{m}^{-1/2}$), by comparing with kinds of literature, this composite can be used in ceramic restoration applications.

REFERENCES

- [1] M. Albakry, M. Guazzato, and M.V. Swain, "Fracture toughness and hardness evaluation of three pressable all-ceramic dental materials", *J. Dent.*, 31(3), 181–188, 2003.
- [2] J. F. Esquivel-Upshaw, K.J. Anusavice, H. Young, J. Jones and C. Gibbs, "Clinical performance of a lithia disilicate-based core ceramic for three unit posterior FPDs", *Int. J. Prosthodontic.*, 17(4), 469–475, 2004.
- [3] C.E. Inglis, "Stress in a plane due to the presence of cracks and sharp corners", *Trans. Inst. Nav. Arch.*, 55 (1), 219–241, 1915.
- [4] A.A. Griffith, "The phenomena of rupture and flow in solids, *Philos.*", *Trans. R. Soc.* 221(6), 163–198, 1920.
- [5] G.R. Irwin, "Fracture dynamics, in: *Fracture of Metals.*", 40A, American Society for Metals., Cleveland, 147–166, 1948.
- [6] D.J. Green, "An Introduction to the Mechanical Properties of Ceramics", University Press, Cambridge, 1998.
- [7] N. Suansuwan and M.V. Swain, "Determination of elastic properties of metal alloys and dental porcelains", *J. Oral Rehabil.*, 28(2), 133–139, 2001.

- [8] W.D. Callister Jr., "Materials Science and Engineering: An Introduction", 5th ed., John Wiley & Sons, Inc., New York, 2000.
- [9] R. Morena, P.E. Lockwood and C.W. Fairhurst, "Fracture toughness of commercial dental porcelains.", *Dent. Mater.* 2(2), 58–62.1986.
- [10] Maji, A. and Choubey, G., "Microstructure and mechanical properties of alumina toughened zirconia (ATZ)", *Materials Today: Proceedings*, 5(2), pp.7457-7465, 2018.
- [11] Carter, C.B. and Norton, M.G. "Ceramic materials: science and engineering", Springer Science & Business Media, 2007.
- [12] Zhang Y and Kim JW., "Graded structures for damage resistant and aesthetic all-ceramic restorations.", *Dent Mater.*, 25(6), 781–790 , 2009.
- [13] Humberto Naoyuki Yoshimura ,Carla Castiglia Gonzaga ,Paulo Francisco Cesar b, Walter Gomes and Miranda Jr.b," Relationship between elastic and mechanical properties of dental ceramics and their index of brittleness.", *Ceramics International*, 38(4) , 4715–4722, 2012.
- [14] Orlovskii, V.P., Komlev, V.S., and Barinov, S.M., "Hydroxyapatite and Hydroxyapatite_Based Ceramics", *Inorg. Mater.*, 38 (7), 973–984, 2002.
- [15] A Balakrishnan, B B Panigrahi, K P Sanosh, Min-Cheol Chu, T N Kim and Seong-Jai Cho," Effect of high thermal expansion glass infiltration on mechanical properties of alumina–zirconia composite.", *Bull. Mater. Sci.*, 32(4), 393–399, 2009.
- [16] Jingchao Zhang, Yunmao Liao, Wei Li ,Yongqi Zhao and Chaoliang Zhang, "Microstructure and mechanical properties of glass-infiltrated Al₂O₃/ZrO₂ nanocomposites.", *J Mater Sci: Mater Med*, 23(3), 239–244, 2012.
- [17] Mohsen Golieskardi, "The Effect of Aluminum Oxide (Al₂O₃) and Cerium Oxide (CeO₂) on the Structural and Mechanical Properties of Ytria Tetragonal Zirconia Polycrystal (Y-TZP).", *Journal of the Australian Ceramic Society* , 51(1), 16-21, 2015.
- [18] J. Fisher, M. Schmid, H. F. Kappert, and J. R. Strub, "Gefugeausbildung der Dentalkeramischen Kemmasse In-Ceram und Thermische Dehnung ihrer Einzelkomponenten.", *Dtsch. Zahnurzt.*, 246, 46143 , 1991.
- [19] B. R. Lawn and D. B. Marshal," Hardness, Toughness, and Brittleness: An Indentation Analysis", *Journal of the American Ceramic Society*, 62(8), 347-350, 1979.
- [20] J.B. Quinn, G.D. Quinn, "Indentation brittleness of ceramics: a fresh approach", *J. Mater. Sci.*, 32(16), 4331–4346, 1997.